A gain-of-function variant in *NNT* causes premature diffuse familial sebaceous hyperplasia

Running head: *NNT* variant causes PDFSH

Lina Liang,[1*] Sheng Wang,[2*] Shimiao Huang,[1] Yonghu Sun,[3] Sha Peng,[1] Christos C. Zouboulis,[4] Amir M. Hossini,[4] Quan Chen,[5†] Huijun Wang,[1†] Zhimiao Lin[1†]

[1]Dermatology Hospital, Southern Medical University, Guangzhou, China

[2]Department of Dermatology, West China Hospital, Sichuan University, Chengdu, China

[3]Shandong Provincial Institute of Dermatology and Venereology, Shandong Academy of Medical Sciences, Jinan, Shandong, China

[4]Departments of Dermatology, Venereology, Allergology and Immunology, Staedtisches Klinikum Dessau, Brandenburg Medical School Theodor Fontane and Faculty of Health Sciences Brandenburg, Dessau, Germany

[5]Department of General Dermatology, Guangzhou Dermatology Hospital, Guangzhou, China

*contributed equally to this work and are joint first authors.

†contributed equally to this work and are joint senior authors.

Corresponding author: Zhimiao Lin

Email: zhimiaolin@bjmu.edu.cn

Acknowledgments: We thank the patients for participating in this study. We also thank Professor Yi Han (Sun Yat-sen University Cancer Center, Guangzhou, China) for valuable technical assistance.

Funding sources: This work was supported by the National Natural Science Foundation of China (grant numbers 82373459 to Z.L. and 82373500 to H.W.).

Conflicts of interest: The authors declare no conflicts of interest except for Christos C. Zouboulis. Christos C. Zouboulis has received honoraria as a consultant for Almirall, Biogen, Boehringer Ingelheim, CLS Behring, Eli Lilly and Company, Estée Lauder, Idorsia, Incyte, L'Oréal, MSD, NAOS-BIODERMA, Novartis, PPM, Sanofi, ShiRhom, Takeda, UCB, and ZuraBio and lecture honoraria from Almirall, Amgen, NAOS-BIODERMA, Biogen, BMS, L'Oréal, Novartis, Pfizer, and UCB. His departments have received grants from his participation as a clinical and research investigator for AstraZeneca, Boehringer Ingelheim, BMS, Brandenburg Medical School Theodor Fontane, EADV, European Union, German Federal Ministry of Education and Research, GSK, Incyte, InflaRx, MSD, Novartis, Relaxera, Sanofi, and UCB. He is President of the EHSF e.V., President of the Deutsches Register Morbus Adamantiades-Behçet e.V., Board member of the International Society for Behçet's Disease, coordinator of the ALLOCATE Skin group of the ERN Skin, and chair of the ARHS Task Force group of the EADV. He is Editor of the EADV News, and co-copyright holder of IHS4 on behalf of the EHSF e.V.

Data availability: The data for this study are available from the authors on reasonable request.

Ethics statement: This study was approved by the Clinical Research Ethics Committee of Dermatology Hospital, Southern Medical University, and was conducted in conformity with the principles of the Declaration of Helsinki.

Patient consent: Written patient consent for publication was obtained.

What is already known about this topic?

- Premature diffuse familial sebaceous hyperplasia (PDFSH) is characterized by the gradual appearance of small, round yellow or flesh-colored papules on the face, often accompanied by hyperseborrhea, typically emerging at or after puberty with a positive family history.
- Nicotinamide nucleotide transhydrogenase (NNT), an inner mitochondrial membrane-bound enzyme, mediates proton gradient-dependent transfer of hydride ion from NADH to $NADP^+$, thereby serving as a principal source of NADPH production. This reduced coenzyme critically sustains cellular redox homeostasis through its antioxidant capacity.
- Enhanced NNT activity has been reported to protect gastric cancer cells from ferroptosis.

What does this study add?

- A missense variant c.2063T>G (p.Leu688Trp) in the *NNT* gene was identified in three unrelated families with PDFSH.
- The *NNT* c.2063T>G variant resulted in elevated NADPH/$NADP^+$ ratio and GSH levels and consequent reduction of ROS in patient's primary keratinocytes and sebaceous gland cells SZ95, leading to enhanced cellular antioxidant capacity.
- Evidences suggesting reduced ferroptosis susceptibility in patients' sebaceous gland were demonstrated. SZ95 sebocytes expressing NNT-Leu688Trp confers resistance to ferroptosis, which might result in the hyperplasia of sebaceous gland in the patients with PDFSH.

What is the translational message?

- We first link a gain-of-function variant in *NNT* to autosomal dominant PDFSH.
- Our study implicates the essential role of NNT in regulating antioxidant capacity and cell survival of sebocytes.

Abstract

Backgrounds Premature diffuse familial sebaceous hyperplasia (PDFSH) constitutes a distinct clinical variant of sebaceous hyperplasia, characterized by three hallmark features: early disease onset, characteristic sparing of perioral and periocular regions, and a positive family history. To date, the pathogenic gene underlying PDFSH remains unidentified.

Objectives The aim of this study was to identify the underlying gene and the pathogenesis of three familial cases with autosomal dominant PDFSH.

Methods Whole-exome sequencing was performed in two unrelated families of autosomal dominant PDFSH. The identified candidate gene was further screened for variants in an additional case using Sanger sequencing. The ultrastructure of sebaceous glands was analyzed by transmission electron microscopy (TEM). Immunofluorescence staining was performed to assess lipid peroxidation levels in sebaceous glands. Functional analyses included quantification of NADPH/$NADP^+$ ratio, glutathione (GSH) levels, and reactive oxygen species (ROS) levels. Flow cytometry with C11-BODIPY and

propidium iodide (PI) staining was performed to assess lipid peroxidation and cell viability, respectively.

Results We identified a missense variant c.2063T>G (p.Leu688Trp) in *NNT* in all affected members across the three PDFSH families. Both patient-derived keratinocytes and NNT-knockdown SZ95 sebocytes overexpressing the mutant nicotinamide nucleotide transhydrogenase (NNT) exhibited enhanced antioxidant capacity, evidenced by elevated $NADPH/NADP^+$ ratio, increased GSH levels, and reduced ROS production compared to controls. Ultrastructural analysis revealed a decreased proportion of mitochondria with cristae disorganization, and immunofluorescence staining showed reduced levels of lipid peroxidation in the patient's sebaceous glands, suggesting decreased ferroptosis susceptibility. *In vitro* experiments confirmed that the *NNT* c.2063T>G variant protects SZ95 sebocytes from ferroptosis through oxidative stress mitigation.

Conclusions We identified a gain-of-function variant c.2063T>G (p.Leu688Trp) in *NNT* underlying PDFSH. This genetic variant enhances antioxidant capacity of NNT while attenuating intracellularly accumulated ROS levels, and reduces sebaceous glands' susceptibility to ferroptosis.

Introduction

Sebaceous gland hyperplasia (SGH), a common benign dermatological entity, is clinically manifested as solitary or clustered yellowish papules. These lesions predominantly arise in sebaceous gland-rich areas of the face, particularly the malar eminences and frontal region. Epidemiologically, SGH demonstrates a predilection for individuals beyond the fifth decade of life.[1] Early-onset manifestations may also occur in several clinical contexts including long-term cyclosporine administration,[2,3] Muir-Torre syndrome,[4] familial cases,[5,6] and X-chromosomal hypohidrotic ectodermal dysplasia.[7]

Premature (or presenile) diffuse familial sebaceous hyperplasia (PDFSH, MIM 601700) is a rare clinical variant of SGH, distinguished by three hallmark features: (1) early onset typically during or soon after puberty, (2) distinctive sparing of the perioral and periocular regions, and (3) evidence of familial clustering.[5,6] While the precise molecular etiology and pathogenic mechanisms of PDFSH are not yet fully characterized, the features of early disease onset and multigenerational disease aggregation strongly suggest constitutional genomic alterations as the underlying cause.

Nicotinamide nucleotide transhydrogenase (NNT), an integral inner mitochondrial membrane protein encoded by the *NNT* gene, serves as a critical antioxidant enzyme by

leveraging a proton gradient to drive NADPH synthesis.[8,9] This reaction involves hydride transfer from NADH to $NADP^+$, generating up to 50% of the mitochondrial NADPH pool essential for redox homeostasis.[8-10] In the cellular defense system against oxidative stress, NNT maintains redox balance by generating NADPH to sustain a high ratio of the reduced glutathione/glutathione disulfide (GSH/GSSG), thereby protecting mitochondria from superoxide anion, hydrogen peroxide, and related reactive oxygen species (ROS) to prevent oxidative damage-induced cell death.[8,11,12] In 2012, Meimaridou *et al.* first reported that *NNT* is the pathogenic gene for familial glucocorticoid deficiency (FGD, MIM 614736).[13] Biallelic loss-of-function variants in *NNT* impair oxidative stress responses, trigger adrenal cell apoptosis, and disrupt steroidogenesis, resulting in FGD.[13,14] In addition, NNT exhibits protumorigenic activity by orchestrating redox homeostasis in multiple solid malignancies, particularly in clinically aggressive subtypes such as non-small cell lung cancer and gastric carcinoma.[10,15]

Ferroptosis is an iron-dependent, non-apoptotic programmed cell death characterized by excessive lipid peroxidation and disrupted redox homeostasis.[16] The process is triggered by ROS-mediated peroxidation cascades, resulting in toxic lipid peroxide accumulation and eventual plasma membrane disintegration.[16] Ultrastructurally, ferroptotic cells usually exhibit characteristic mitochondrial changes including shrinkage, cristae disorganization, and outer membrane rupture.[11,17] Emerging evidence has

implicated the crucial roles of ferroptosis in sebaceous gland biology, with recent studies showing that photothermal therapy for acne vulgaris reduces sebum secretion through induction of sebocyte ferroptosis.[18]

Here, we identify a missense variant c.2063T>G (p.Leu688Trp, rs1313691502) in the *NNT* gene as the genetic basis for autosomal dominant PDFSH in three unrelated families. We demonstrated that the *NNT* variant exerts a gain-of-function property, conferring ferroptosis resistance in sebocytes through ROS suppression. This mechanism may underlie the development of NNT-associated sebaceous hyperplasia.

Patients and methods

Participants

Three unrelated families (Fam1-Fam3) were included in the study. Written informed consent was obtained from all participants. This study was approved by the Clinical Research Ethics Committee of the Dermatology Hospital, Southern Medical University.

Cell culture

Lesional skin specimens were obtained followed by subcutaneous fat excision. Tissues were disinfected sequentially with povidone-iodine and 75% ethanol, then mechanically

minced into < 2mm fragments. Epidermal-dermal separation was achieved by incubating the tissue in 2.5 mg/mL dispase II at 4°C for 14-16 hours. Isolated epidermis was enzymatically dissociated using 0.25% trypsin at 37°C for 5-10 min, followed by neutralization and gentle trituration. Cell suspensions were centrifuged, resuspended in keratinocyte growth medium, and plated on cell culture dish containing coating maintained at 37°C with 5% CO_2.

The immortalized human sebaceous gland cell line SZ95[19] was cultured in Sebomed® basal medium (Sigma-Aldrich, F8205) supplemented with 5 ng/mL human epidermal growth factor (PeproTech, AF-100-15) and 10% fetal bovine serum (Gibco) at 37°C with 5% CO_2.

Generation of NNT-overexpressing SZ95 cell Lines

Firstly, NNT-knockdown SZ95 sebocytes were generated by lentiviral transduction using *NNT*-specific shRNA (GeneCopoeia, LPP-HSH097229-LVRU6H), followed by hygromycin B selection. For exogenous NNT expression, CMV promoter-driven lentiviral vectors expressing short hairpin RNA (shRNA)-resistant (r) human *NNT* cDNA (NM_012343.3) with C-terminal 3×Flag tags was generously provided by Dr Han.[20] The NNT-Leu688Trp variant (rNNT-Leu688Trp) was obtained by site-directed mutagenesis. The recombinant lentiviral plasmids were co-transfected with packaging plasmids

(psPAX2 and pMD2.G) into HEK293T cells to generate replication-incompetent lentiviral particles. Stable NNT-overexpressing cell lines were generated by transducing NNT-knockdown SZ95 sebocytes with lentiviral particles, followed by puromycin selection. Control cell lines were established using empty vector (EV) lentivirus under identical conditions.

NADPH/NADP$^+$, GSH and ROS detection assay

Intracellular NADPH/NADP$^+$ and GSH levels in the primary keratinocytes or SZ95 sebocytes were quantified using the NADP/NADPH-Glo Bioluminescent Assay kit (Promega, G9082) and GSH-Glo Glutathione Assay kit (Promega, V6911) following the manufacturer's protocol.

Intracellular ROS levels were quantified using the peroxide-sensitive fluorescent probe 2',7'-dichlorodihydrofluorescein diacetate (DCFH-DA). Briefly, primary keratinocytes or SZ95 sebocytes were seeded in 6-well plates at a density of 200,000 cells per well. After reaching confluence, the cells were washed twice with PBS, trypsinized, and washed once more with PBS. The cells were then incubated with 10 μM DCFH-DA at 37°C for 30 min. Following three washes with PBS, cells were resuspended in 500 μL PBS and analyzed for fluorescence intensity on BD Celesta flow cytometer with an excitation wavelength of 488nm. Data were analyzed using FlowJo v10 software.

Results

Clinical and histopathologic manifestations of the patients

Three unrelated Chinese families with autosomal dominant PDFSH were enrolled in this study (Figure 1d). All affected individuals developed multiple yellowish papules on the face at or after puberty (onset age ranging from 16 to 35 years), with a progressive increase in lesion number. Physical examination revealed multiple coalesced 1-5 mm yellowish to flesh-colored papules and plaques predominantly localized to the forehead and cheeks, with additional scattered lesions observed behind the ears, on the neck, and on the upper chest, sparing the perioral and periorbital regions (Figures 1a, b and S1a-d). Most patients reported facial greasiness. Histopathological analysis of the skin lesions from the probands of three families (Fam1:III-2, Fam2:II-2 and Fam3:II-1) demonstrated abnormal hypertrophic sebaceous glands in the upper dermis composed of abundant mature sebocytes and infiltration of sparse inflammatory cells in the superficial dermis (Figure 1c).

Ultrastructural features of the skin lesion

Ultrastructural examination of sebaceous glands from patient Fam2:II-2 and a healthy control was performed using transmission electron microscopy (TEM). Terminally

differentiated sebocytes from healthy control displayed mitochondria structural changes with cristae disorganization and loss of outer membrane integrity (Figure 2a), recapitulating the characteristic mitochondrial dysfunction patterns observed in ferroptotic cells.[11,17] In contrast, terminally differentiated sebocytes from Fam2:II-2 displayed a significantly lower proportion of mitochondria with cristae disorganization compared to the control (Figure 2a, b). The morphological preservation suggests enhanced resistance to ferroptotic stress in the patient cells.

Identification of the *NNT* variant in patients

For WES data, we focused on rare (MAF < 0.001), heterozygous non-synonymous variants in the same candidate gene present in all the four affected individuals (Fam1:II-2, Fam1:III-2, Fam1:III-3 and Fam2:II-2). A variant c.2063T>G (p.Leu688Trp, NM_012343.3) in the *NNT* gene was identified in all the four affected individuals, which was validated by Sanger sequencing (Figure 2c). We further performed Sanger sequencing on the family members of Fam1, Fam2 and Fam3. Interestingly, we found that Fam3:II-1 and Fam3:II-2 harbored the same variant c.2063T>G in *NNT*. The *NNT* c.2063T>G variant was confirmed to co-segregate with the phenotype in all enrolled family members (Figure 1d) except Fam1:IV-1 who harbored the *NNT* variant but had not SGH. Given Fam1:IV-1 was only 16 years old and the onset of the disorder in other family members was around 20 years old, we assumed that Fam1:IV-1 might develop the

phenotype in a few years. Notably, the residue Leu688, which is located in the membrane domain (dII) of NNT, is highly conserved across species (Figure 2d) and was predicted to be "disease causing" *in silico* (https://www.mutationtaster.org). This variant is present in gnomAD in an extremely low frequency of 0.000003100 (5 in 1612868) but absent in East Asian.

The c.2063T>G variant enhanced the antioxidant capacity of NNT

NNT maintains mitochondria redox homeostasis by regenerating NADPH, which is essential for glutathione peroxidase-mediated GSSG reduction to GSH, thereby enabling efficient ROS detoxification.[12] To initially assess the functional impact of the *NNT* c.2063T>G variant, we assessed the $NADPH/NADP^+$ ratio, GSH levels, and ROS levels in primary keratinocytes derived from Fam2:II-2 and a healthy control. The results showed that $NADPH/NADP^+$ ratio and GSH levels were significantly upregulated in the primary keratinocytes from Fam2:II-2 compared to those of the control (Figure 3a, b). Consistently, the ROS levels were significantly reduced in the keratinocytes from Fam2:II-2 (Figure 3c).

To further clarify the role of the *NNT* c.2063T>G variant in sebocytes, we overexpressed rNNT-WT and rNNT-Leu688Trp in NNT-knockdown SZ95 sebocytes (Figure S3e) and assessed $NADPH/NADP^+$ ratio, GSH levels, and ROS levels in each

group. To minimize interference from endogenous NNT in SZ95 sebocytes, which exhibit high baseline NNT expression, we established stable NNT-knockdown SZ95 sebocytes. Western blot analysis confirmed > 90% reduction in endogenous NNT protein levels compared to scramble shRNA control (Figure S3d). The cells overexpressing rNNT-Leu688Trp exhibited significantly elevated NADPH/$NADP^+$ ratio and GSH levels compared to the cells overexpressing rNNT-WT (Figure 3d, e), accompanied by a marked reduction in ROS levels (Figure 3f), indicating that the *NNT* c.2063T>G variant enhances the intracellular antioxidant capacity of NNT. Furthermore, consistent with *in vivo* data, we also observed different ultrastructural mitochondrial changes between SZ95 sebocytes transfected with rNNT-WT and rNNT-Leu688Trp treated with RSL3, a specific ferroptosis inducer. After treatment, cells expressing rNNT-WT exhibited extensive mitochondria with cristae disorganization (Figure S2a)—ultrastructural features characteristic of ferroptosis and mirroring the mitochondrial alterations seen in terminally differentiated sebocytes *in vivo*. In contrast, SZ95 sebocytes expressing rNNT-Leu688Trp showed a marked reduction in the proportion of such mitochondria (Figure S2a, b), further suggesting that the *NNT* c.2063T>G variant enhances ferroptosis resistance in sebocytes.

To exclude the possibility that functional changes are due to altered protein abundance of NNT, we performed qPCR and Western blot using primary keratinocytes from patient

Fam2:II-2 and a healthy control. As shown in Figures S3a and S3b, qPCR and Western blot analysis revealed no significant differences between the patient and healthy control, suggesting that the variant did not affect the transcription and translation of *NNT*. Similarly, Western blot was performed in NNT-knockdown SZ95 sebocytes overexpressing rNNT-Leu688Trp and those overexpressing rNNT-WT, which revealed comparable protein abundance of NNT (Figure S3d, e).

Lipid peroxidation reduced in PDFSH patients

Ferroptosis is an iron-dependent cell death pathway characterized by ROS accumulation leading to excessive lipid peroxidation and cell death.[11] In ferroptosis, mitochondria exhibit distinct morphological alterations, including outer membrane rupture and reduced or disorganized mitochondrial cristae.[21] Notably, our ultrastructural analysis of normal sebaceous glands revealed frequent mitochondria with cristae disorganization in terminally differentiated sebocytes, a morphology consistent with ferroptosis-associated changes, whereas patient tissues showed a remarkable decrease in mitochondria with cristae disorganization (Figure 2a, b). Given prior evidence that enhanced NNT activity confers ferroptosis resistance in gastric cancer,[20] we hypothesized that the *NNT* c.2063T>G variant also enhances resistance to ferroptosis in sebocytes, thereby reducing their susceptibility to ferroptosis. To test this, we assessed the expression of 4-HNE, a key lipid peroxidation marker, by immunofluorescence in lesional skin from two

patients (Fam1:III-2 and Fam2:II-2) and two healthy controls. A significant decrease in the levels of 4-HNE in patients (Figure 4a, b) was detected compared to controls, suggesting reduced ferroptosis susceptibility in sebaceous glands.

NNT c.2063T>G variant conferred ferroptosis resistance in SZ95 sebocytes

To determine whether the *NNT* c.2063T>G variant confers ferroptosis resistance in sebocytes, we analyzed lipid peroxidation and cell death in NNT-knockdown SZ95 sebocytes expressing EV, rNNT-WT, or rNNT-Leu688Trp. Cells were treated with the ferroptosis inducer RSL3, with or without the antioxidant N-acetylcysteine (NAC). Under basal conditions, all groups exhibited comparable lipid peroxidation levels and viability (Figure 5a-d). RSL3 exposure triggered pronounced lipid peroxidation and cell death in EV-transfected cells, while cells expressing rNNT-WT showed partial mitigation of these effects (Figure 5a-d), indicating that NNT can mitigate RSL3-induced ferroptosis in SZ95 sebocytes. Remarkably, compared to the cells expressing rNNT-WT, cells expressing rNNT-Leu688Trp demonstrated substantially attenuated lipid peroxidation and superior survival (Figure 5a-d), indicating enhanced ferroptosis resistance conferred by the Leu688Trp variant.

Notably, NAC co-treatment abolished RSL3-induced lipid peroxidation and cell death in all groups (Figure 5a-d), confirming oxidative stress as the primary driver of

ferroptosis. Together with our findings that the variant significantly enhances NNT-mediated antioxidant capacity, these results suggest that the *NNT* c.2063T>G (p.Leu688Trp) variant markedly increases sebocytes resistance to ferroptosis through oxidative stress mitigation.

Discussion

In this study, we identified *NNT* as a causative gene for PDFSH. We demonstrate that a gain-of-function variant in *NNT* enhances resistance to ferroptosis in sebocytes, contributing to the pathogenesis of SGH. NNT serves as a pivotal mitochondrial enzyme, generating NADPH through proton gradient coupling.[8,9] This mitochondrial NADPH pool sustains GSH redox cycling, a critical defense mechanism against ROS that governs cellular survival.[12] Consistently, *nnt-1* deletion mutants in *Caenorhabditis elegans* exacerbate oxidative stress susceptibility via impaired GSH/GSSG ratio,[22] while NNT-knockdown in human PC12 cells disrupts redox homeostasis through NADPH depletion, GSH imbalance, and H_2O_2 accumulation.[23] In FGD, biallelic loss-of-function variants in *NNT* cause oxidative dysregulation characterized by GSH depletion, ROS accumulation, and cell death,[13,14,24] underscoring essential roles of NNT in oxidative defense. In contrast, our patient-derived primary keratinocytes showed an increase of NADPH/$NADP^+$ ratio and GSH levels with concomitant ROS reduction compared to the

healthy control. Similarly, NNT-knockdown SZ95 sebocytes expressing the rNNT-Leu688Trp showed a higher NADPH/$NADP^+$ ratio, elevated GSH levels, and decreased ROS levels compared to cells expressing rNNT-WT. These data collectively demonstrate that the c.2063T>G variant enhances NNT catalytic efficiency to regulate redox homeostasis, thus exerting a gain-of-function property.

NNT comprises three functional domains: the NAD(H)-binding domain (dI), the transmembrane proton channel domain (dII), and the NADP(H)-binding domain (dIII). Mutagenesis studies in *E. coli* have demonstrated that alanine or cysteine substitutions at conserved residues Ser250, Ser251, or Ser256 of *E. coli* (homologous to human NNT Ser867, Ser868, and Ser873) within transmembrane helix 14 (TM14) of the dII enhance NNT activity.[25,26] This functional enhancement may occur through induced conformational changes at the dIII-dII interface (facilitated by their spatial proximity) or through structural modulation of key transmembrane helices in the central dII.[25-27] These structural alterations may either optimize NADP(H)-binding dynamics via allosteric coupling to enhance catalytic efficiency or stabilize the open state of the proton channel in dII, thereby improving proton translocation efficiency.[25-27] Residue 688 is located within TM8 of dII, spatially proximal to the dIII-dII interface. The Leu688Trp substitution replaces the wild-type hydrophobic aliphatic residue leucine with a tryptophan residue that harbors a rigid indole ring. This substitution is likely to strengthen

aromatic interactions (residues Phe, Trp, and Tyr), particularly π-π stacking, which are critical for protein folding, thermal stability, and conformational regulation of transmembrane proteins.[28-30] We hypothesize that the Leu688Trp substitution might optimize the dIII-dII interface or stabilize the open conformation of the proton channel to improve the coupling efficiency between NADPH production and proton translocation, leading to gain-of-function changes. A representative example of such a mechanism is *KCNC2*, which encodes the voltage-gated potassium (K^+) channel subunit Kv3.2. The Cys125Tyr substitution, located near the α-6 helix of the cytoplasmic tetramerization domain—a key regulator of channel gating—introduces a phenol side chain that forms π-π stacking interactions with Tyr156.[30] This interaction stabilizes the open conformation of the channel, leading to a significant hyperpolarizing shift in voltage-dependent activation, which represents a distinct gain-of-function phenotype.[30] Further functional studies are warranted to demonstrate the conformational changes and functional alterations of NNT by Leu688Trp substitution.

NNT critically promotes tumor progression by maintaining redox homeostasis and Fe-S protein function.[10,15,20] In gastric cancer, Han *et al.* demonstrated that enhanced NNT activity protects tumor cells from ferroptosis through Fe-S cluster stabilization, highlighting NNT as a key ferroptosis modulator.[20] Ferroptosis is regulated by oxidative stress and antioxidant capacity, in which ROS-driven lipid peroxidation generates

cytotoxic products such as 4-HNE.[11,21,31] Our TEM analysis revealed reduced ferroptosis-associated mitochondrial ultrastructures in terminally differentiated sebocytes in the patient with PDFSH. Consistently, the patients' skin lesion exhibited reduced 4-HNE levels, together suggesting decreased susceptibility to ferroptosis. NNT-knockdown SZ95 sebocytes expressing rNNT-Leu688Trp showed enhanced antioxidant capacity and resistance to RSL3-induced ferroptosis. Co-treatment with NAC completely reversed RSL3-induced ferroptosis. These results implicate that the *NNT* c.2063T>G variant confers sebocytes resistance to ferroptosis through oxidative stress mitigation. A recent study has revealed that near-infrared radiation (NIR), which induces intracellular ROS elevation,[32] triggers ferroptosis in sebocytes[18]—suggesting ferroptosis mediates stress-induced sebocyte death. Thus, we hypothesize that *NNT* c.2063T>G variant primarily confers protection against sebocyte ferroptosis under stressful conditions (e.g., solar exposure including UV, visible light, and NIR). This protection likely elevates the ferroptosis resistance threshold, postponing the death of mature sebocytes and leading to slow progressive accumulation of mature sebocytes in the sebaceous gland. This phenomenon of postponed cell death causing sebocyte accumulation parallels the findings of Atsugi *et al.*, where tight junction barrier defects impaired mature sebocyte degradation during holocrine secretion, leading to accumulated incompletely degenerated sebocytes in sebaceous ducts.[33]

Notably, cutaneous biology studies have demonstrated that sebaceous glands inherently sustain elevated NADPH concentrations relative to adjacent epidermal compartments.[34,35] This is further demonstrated by our immunohistochemical analysis showing pronounced NNT immunoreactivity in sebaceous units compared to interfollicular epidermis (Figure S3c). It's tempting to assume that NADPH-dependent redox maintenance exerts greater functional significance in sebaceous glands than interfollicular epidermis, which is further supported by the fact that the gain-of-function variant in *NNT* causes sebaceous gland-specific phenotype of PDFSH, rather than epidermal differentiation disorders.

In summary, we identify a gain-of-function *NNT* variant as a cause of PDFSH through enhanced ferroptosis resistance of sebocytes. Our study not only expands the *NNT*-associated disease spectrum, but also paves a new avenue for developing future therapeutic interventions for SGH.

References

1. Hou X, Wei Z, Zouboulis CC*, et al.* Aging in the sebaceous gland. *Frontiers in Cell and Developmental Biology.* 2022;10.
2. Boschnakow A, May T, Assaf C*, et al.* Ciclosporin A-induced sebaceous gland hyperplasia. *Br J Dermatol.* 2003;149:198-200.
3. Engel F, Ellero B, Woehl-Jaegle ML*, et al.* Hyperplasies sébacées profuses du visage induites par la ciclosporine. *Annales de Dermatologie et de Vénéréologie.* 2005;132:342-345.

4. Marcusson JA, Bjarnason B, Ros AM. Isotretinoin for sebaceous skin lesions in Muir-Torre syndrome: a case report. *Acta Derm Venereol.* 1998;78:479-480.
5. Boonchai W, Leenutaphong V. Familial presenile sebaceous gland hyperplasia. *J Am Acad Dermatol.* 1997;36:120-122.
6. Liu YCS, Cheng YP, Liu CI, *et al.* Presenile diffuse familial sebaceous hyperplasia successfully treated with low-dose isotretinoin: A report of two cases and review of the published work. *The Journal of Dermatology.* 2016;43:1205-1208.
7. Piletta PA, Calza AM, Masouyé I, *et al.* Hypohidrotic ectodermal dysplasia with recurrent otitis and sebaceous gland hypertrophy of the face. *Dermatology.* 1995;191:355-358.
8. Hoek JB, Rydström J. Physiological roles of nicotinamide nucleotide transhydrogenase. *Biochem J.* 1988;254:1-10.
9. Kampjut D, Sazanov LA. Structure and mechanism of mitochondrial proton-translocating transhydrogenase. *Nature.* 2019;573:291-295.
10. Ward NP, Kang YP, Falzone A, *et al.* Nicotinamide nucleotide transhydrogenase regulates mitochondrial metabolism in NSCLC through maintenance of Fe-S protein function. *J Exp Med.* 2020;217.
11. Tang D, Chen X, Kang R, *et al.* Ferroptosis: molecular mechanisms and health implications. *Cell Research.* 2020;31:107-125.
12. Circu ML, Aw TY. Reactive oxygen species, cellular redox systems, and apoptosis. *Free Radical Biology and Medicine.* 2010;48:749-762.
13. Meimaridou E, Kowalczyk J, Guasti L, *et al.* Mutations in NNT encoding nicotinamide nucleotide transhydrogenase cause familial glucocorticoid deficiency. *Nature Genetics.* 2012;44:740-742.
14. Bodoni AF, Coeli-Lacchini FB, Gebenlian JL, *et al.* Nicotinamide Nucleotide Transhydrogenase Is Essential for Adrenal Steroidogenesis: Clinical and In Vitro Lessons. *The Journal of Clinical Endocrinology & Metabolism.* 2023;108:1464-1474.
15. Li S, Zhuang Z, Wu T, *et al.* Nicotinamide nucleotide transhydrogenase-mediated redox homeostasis promotes tumor growth and metastasis in gastric cancer. *Redox Biology.* 2018;18:246-255.
16. Chen X, Kang R, Kroemer G, *et al.* Organelle-specific regulation of ferroptosis. *Cell Death Differ.* 2021;28:2843-2856.
17. Dixon SJ, Olzmann JA. The cell biology of ferroptosis. *Nat Rev Mol Cell Biol.* 2024;25:424-442.
18. Wu R, Li J, Tian H, *et al.* Unveiling the mechanism of photothermal therapy in acne man-agement: targeting sebaceous gland ferroptosis via umbilical cord mesenchymal stem cell membrane-encapsulated Au-Ag-PDA. *Front Bioeng Biotechnol.* 2024;12:1426477.
19. Zouboulis CC, Seltmann H, Neitzel H, *et al.* Establishment and characterization of an immortalized human sebaceous gland cell line (SZ95). *J Invest Dermatol.* 1999;113:1011-

1020.
20. Han Y, Zhang Y-Y, Pan Y-Q, *et al.* IL-1β-associated NNT acetylation orchestrates iron-sulfur cluster maintenance and cancer immunotherapy resistance. *Molecular Cell.* 2023;83:1887-1902.e1888.
21. Liu Ye, Lu S, Wu L-l, *et al.* The diversified role of mitochondria in ferroptosis in cancer. *Cell Death & Disease.* 2023;14.
22. Arkblad EL, Tuck S, Pestov NB, *et al.* A Caenorhabditis elegans mutant lacking functional nicotinamide nucleotide transhydrogenase displays increased sensitivity to oxidative stress. *Free Radical Biology and Medicine.* 2005;38:1518-1525.
23. Yin F, Sancheti H, Cadenas E. Silencing of nicotinamide nucleotide transhydrogenase impairs cellular redox homeostasis and energy metabolism in PC12 cells. *Biochimica et Biophysica Acta (BBA) - Bioenergetics.* 2012;1817:401-409.
24. Weinberg-Shukron A, Abu-Libdeh A, Zhadeh F, *et al.* Combined mineralocorticoid and glucocorticoid deficiency is caused by a novel founder nicotinamide nucleotide transhydrogenase mutation that alters mitochondrial morphology and increases oxidative stress. *Journal of Medical Genetics.* 2015;52:636-641.
25. Yamaguchi M, Stout CD, Hatefi Y. The proton channel of the energy-transducing nicotinamide nucleotide transhydrogenase of Escherichia coli. *J Biol Chem.* 2002;277:33670-33675.
26. Karlsson J, Althage M, Rydström J. Roles of individual amino acids in helix 14 of the membrane domain of proton-translocating transhydrogenase from Escherichia coli as deduced from cysteine mutagenesis. *Biochemistry.* 2003;42:6575-6581.
27. Yamaguchi M, Stout CD. Essential glycine in the proton channel of Escherichia coli transhydrogenase. *J Biol Chem.* 2003;278:45333-45339.
28. Meyer EA, Castellano RK, Diederich F. Interactions with aromatic rings in chemical and biological recognition. *Angew Chem Int Ed Engl.* 2003;42:1210-1250.
29. Duan J, Li Z, Li J, *et al.* Structure of full-length human TRPM4. *Proc Natl Acad Sci U S A.* 2018;115:2377-2382.
30. Clatot J, Currin CB, Liang Q, *et al.* A structurally precise mechanism links an epilepsy-associated KCNC2 potassium channel mutation to interneuron dysfunction. *Proc Natl Acad Sci U S A.* 2024;121:e2307776121.
31. Wang B, Wang Y, Zhang J, *et al.* ROS-induced lipid peroxidation modulates cell death outcome: mechanisms behind apoptosis, autophagy, and ferroptosis. *Arch Toxicol.* 2023;97:1439-1451.
32. Barolet D, Christiaens F, Hamblin MR. Infrared and skin: Friend or foe. *J Photochem Photobiol B.* 2016;155:78-85.
33. Atsugi T, Yokouchi M, Hirano T, *et al.* Holocrine Secretion Occurs outside the Tight Junction Barrier in Multicellular Glands: Lessons from Claudin-1-Deficient Mice. *J Invest Dermatol.* 2020;140:298-308.e295.

34. Im MJ, Hoopes JE. Enzymes of carbohydrate metabolism in normal human sebaceous glands. *J Invest Dermatol.* 1974;62:153-160.
35. Im MJ, Hoopes JE. Quantitative histochemistry of nicotinamide adenine nucleotides in human skin. *J Invest Dermatol.* 1970;55:277-281.

Figure Legend

Figure 1. Clinical, histopathologic features and pedigrees of three families with PDFSH.

(a-b) Multiple pale yellow to flesh-colored papules on the face, sparing periocular and perioral regions. Some lesions show central umbilication and mild erythema at the base in Fam2:II-2 (a) and Fam1:III-2 (b).

(c) Histopathology of Fam1:III-2 shows increased hypertrophic sebaceous glands localized in the superficial dermis, containing abundant mature sebocytes, with infiltration of inflammatory cells in the superficial dermis. Scale bar = 250μm.

(d) Pedigrees of the autosomal-dominant PDFSH were analyzed in the study. Filled symbols indicate affected individuals with PDFSH. Arrows denote probands. Black stars denote individuals whose DNA samples were obtained.

Figure 2. Ultrastructural features and Sanger sequencing.

(a) Transmission electron microscopy (TEM) of terminally differentiated sebaceous glands between healthy control and Fam2:II-2. Yellow stars denote mitochondria with cristae disorganization. Scale bars = 5μm.

(b) Quantitative analysis revealed a marked decrease in the proportion of mitochondria with cristae disorganization in the patient Fam2:II-2 compared to the healthy control. Error bars represent SEM; two-tailed Student's t-test; **p<0.01.

(c) Sanger sequencing showed the *NNT* c.2063T>G variant in the affected individuals.

(d) Sequence alignment showed that the affected residue Leu688 in NNT is highly conserved across species.

Figure 3. Redox imbalance in patient-derived keratinocytes and NNT-knockdown SZ95 sebocytes.

(a-c) Primary keratinocytes from patient Fam2:II-2 and healthy control were measured, including (a) NADPH/$NADP^+$ ratio, (b) glutathione (GSH) levels, and (c) relative reactive oxygen species (ROS) levels. n = 3 replicates. Error bars represent SEM; two-tailed Student's t-test; *p<0.05, **p<0.01.

(d-f) (d) NADPH/$NADP^+$ ratio, (e) GSH levels, and (f) relative ROS levels were analyzed in NNT-knockdown SZ95 sebocytes expressing either empty vector (EV), short hairpin RNA (shRNA)-resistant (r) wild-type NNT (rNNT-WT), or the NNT-Leu688Trp variant (rNNT-Leu688Trp). n = 3 replicates. Error bars represent SEM; one-way ANOVA; *p<0.05, **p<0.01.

Figure 4. Lipid peroxidation in sebaceous glands.

(a-b) Immunofluorescence staining of the lipid peroxidation marker 4-HNE showed reduced levels in sebaceous glands of the skin sections from Fam1:III-2 (a) and Fam2:II-2 (b) in comparison to two healthy controls. Scale bars = 100μm.

Figure 5. The *NNT* c.2063T>G variant mitigates ferroptosis in SZ95 sebocytes.

(a-b) Lipid peroxidation analysis in NNT-knockdown SZ95 sebocytes expressing EV, rNNT-WT, or rNNT-Leu688Trp, followed by treatment with 0.4μM RSL3 for 6 h. Representative images (a) and quantification data are shown (b). n = 3 replicates. Error bars represent SEM; one-way ANOVA; **p<0.01; ns, not significant.

(c-d) Images (c) and flow cytometry quantification (d) of PI staining in NNT-knockdown SZ95 sebocytes expressing EV, rNNT-WT, or rNNT-Leu688Trp, followed by treatment with 0.5μM RSL3 for 6 h. n = 3 replicates. Error bars represent SEM; one-way ANOVA;

**p<0.01; ns, not significant.

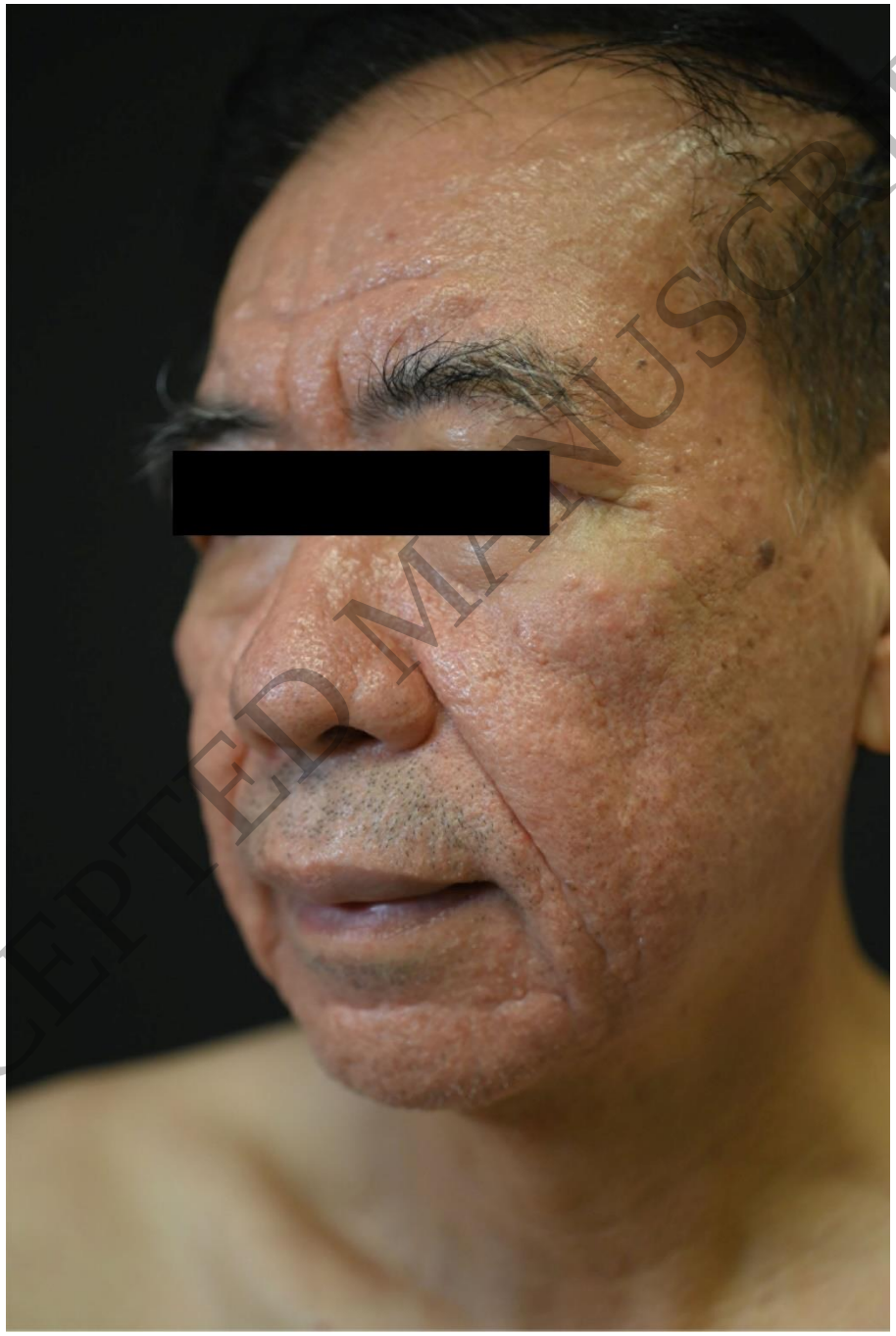

Figure 1a

119x179 mm (DPI)

Figure 1b

147x79 mm (DPI)

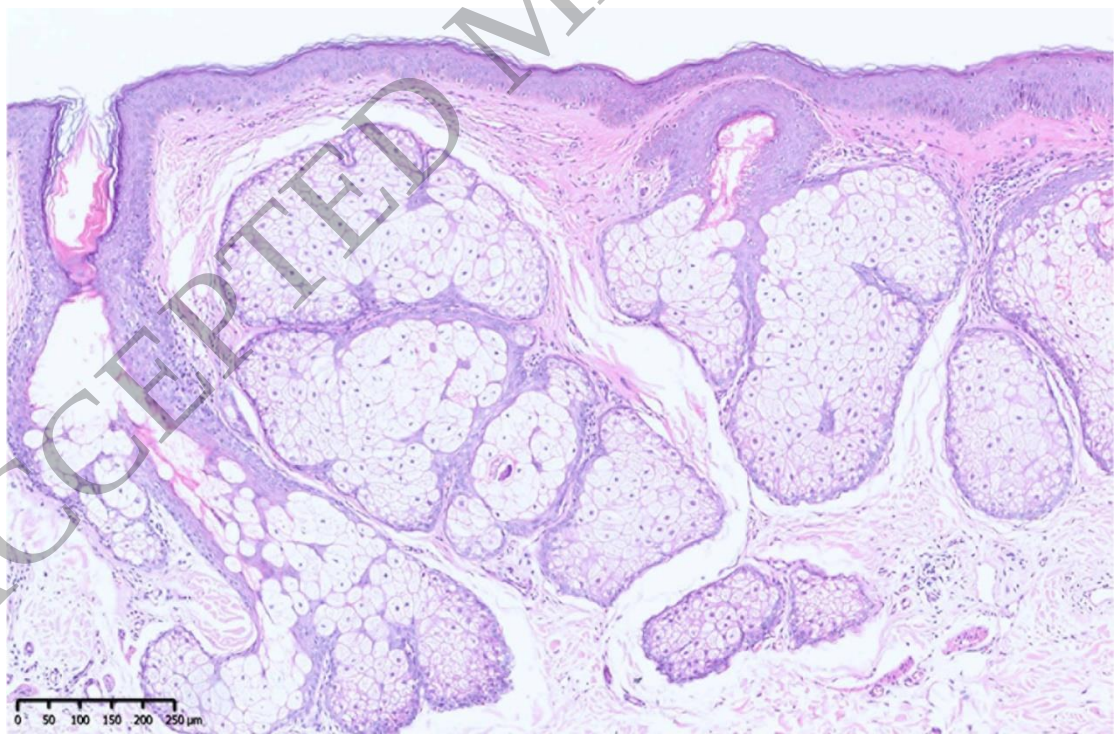

Figure 1c

147x96 mm (DPI)

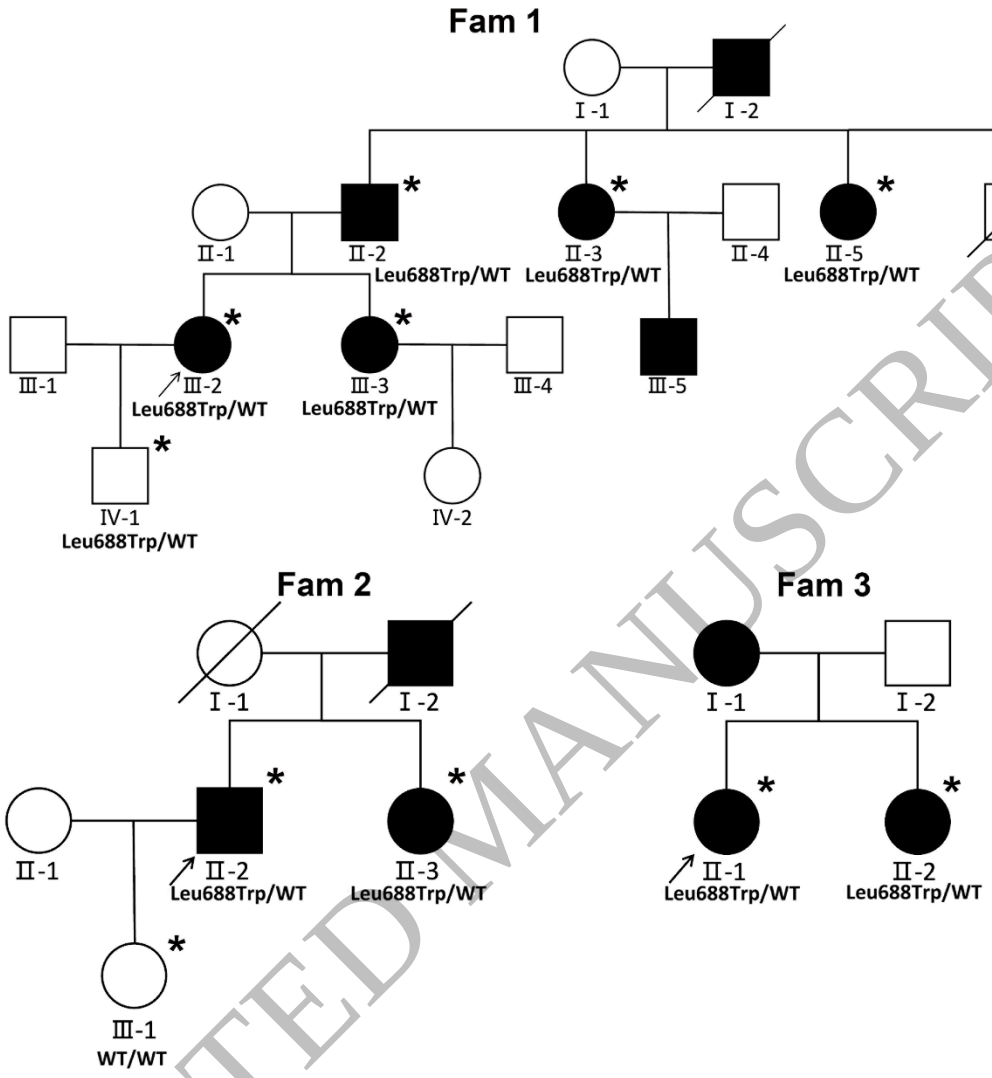

Figure 1d

147x143 mm (DPI)

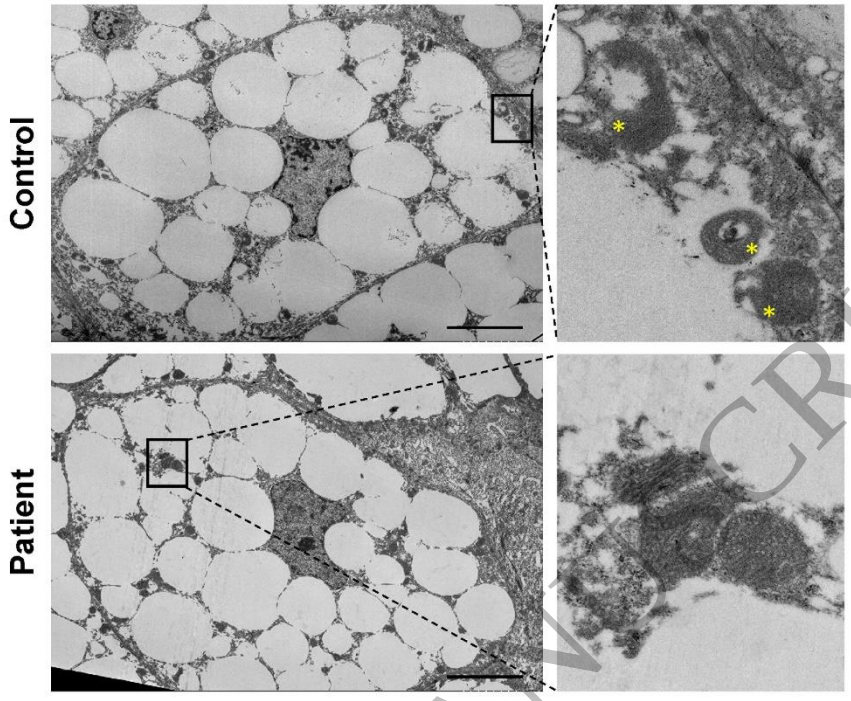

Figure 2a

117x97 mm (DPI)

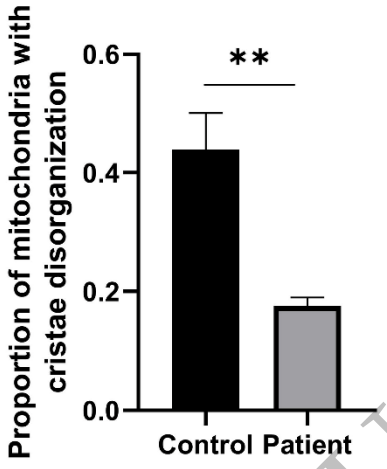

Figure 2b

56x97 mm (DPI)

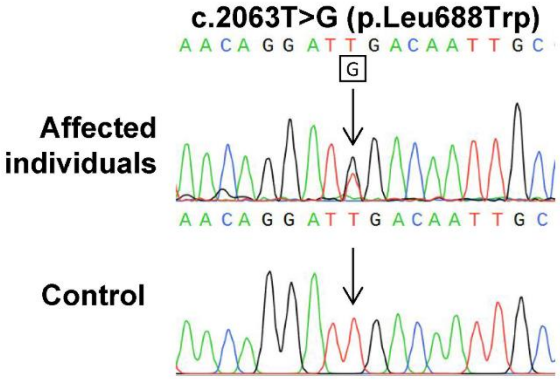

Figure 2c

75x62 mm (DPI)

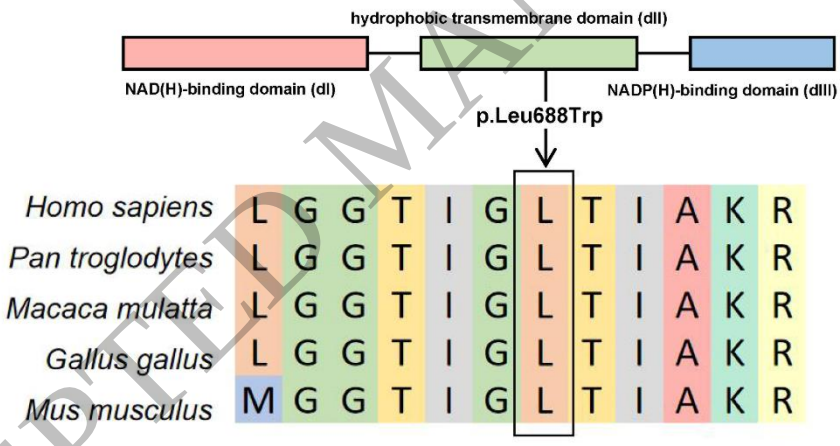

Figure 2d

114x62 mm (DPI)

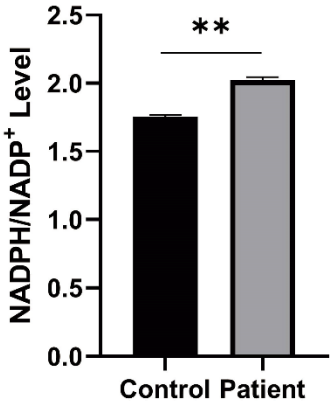

Figure 3a

51x60 mm (DPI)

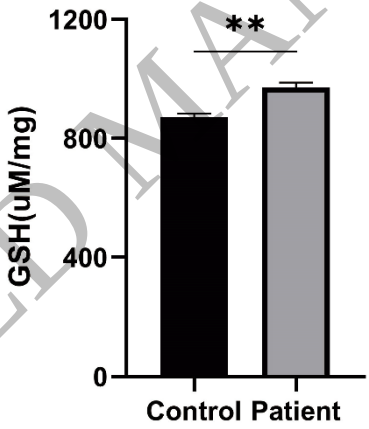

Figure 3b

53x60 mm (DPI)

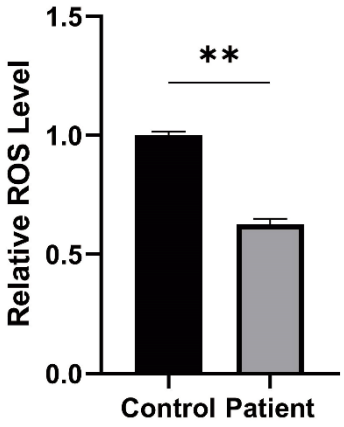

Figure 3c

50x60 mm (DPI)

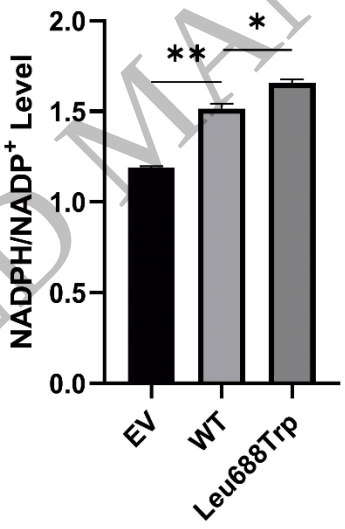

Figure 3d

51x74 mm (DPI)

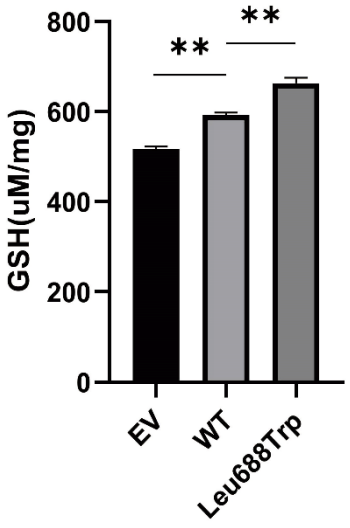

Figure 3e

53x74 mm (DPI)

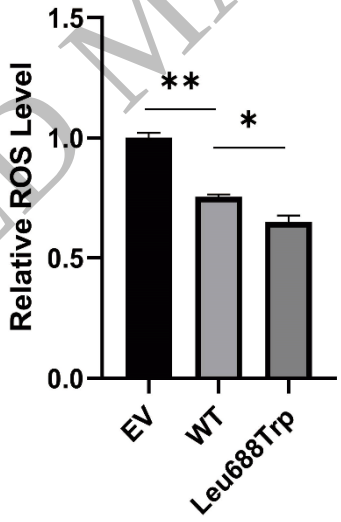

Figure 3f

50x74 mm (DPI)

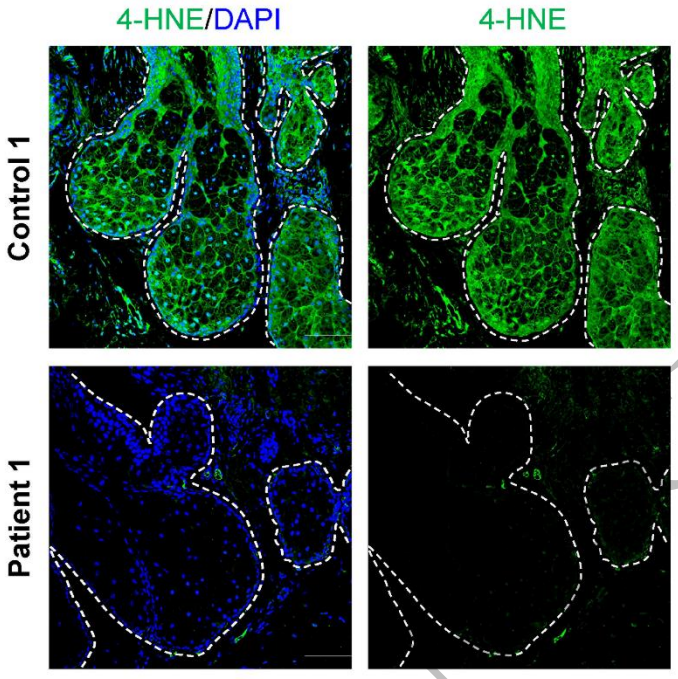

Figure 4a

94x94 mm (DPI)

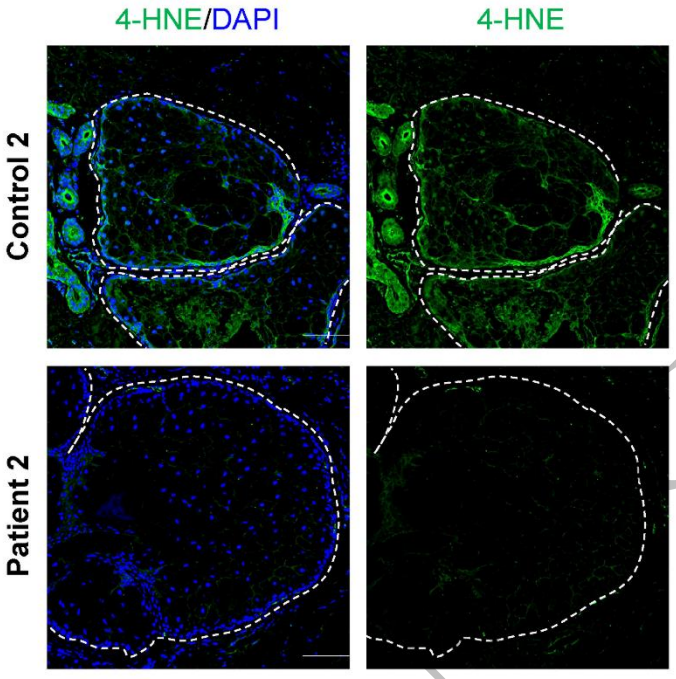

Figure 4b

94x94 mm (DPI)

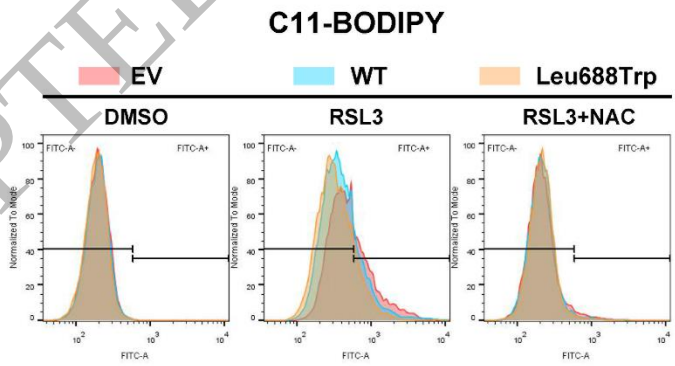

Figure 5a

93x53 mm (DPI)

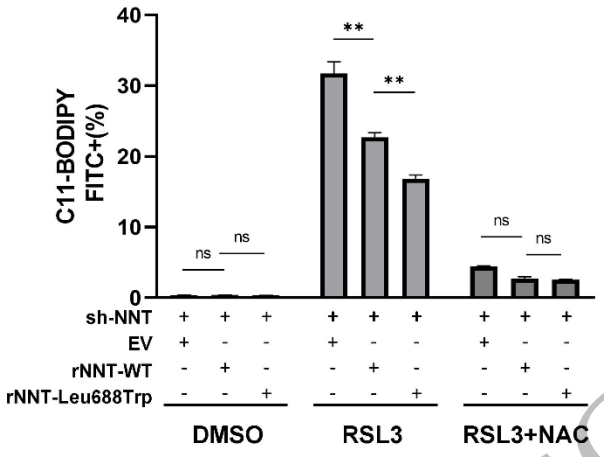

Figure 5b

85x64 mm (DPI)

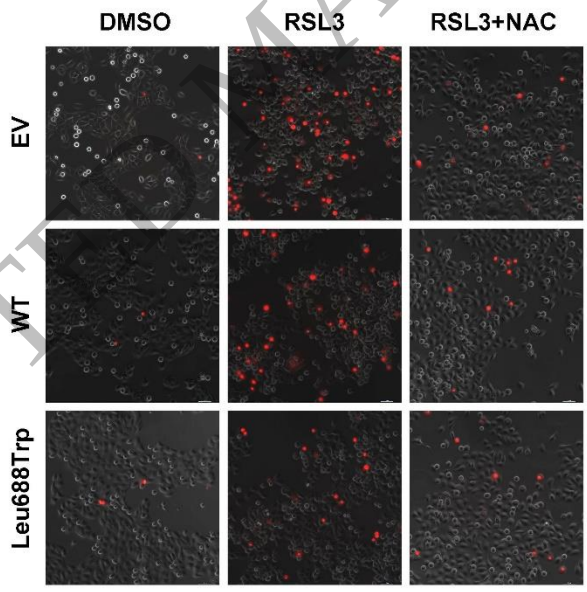

Figure 5c

82x82 mm (DPI)

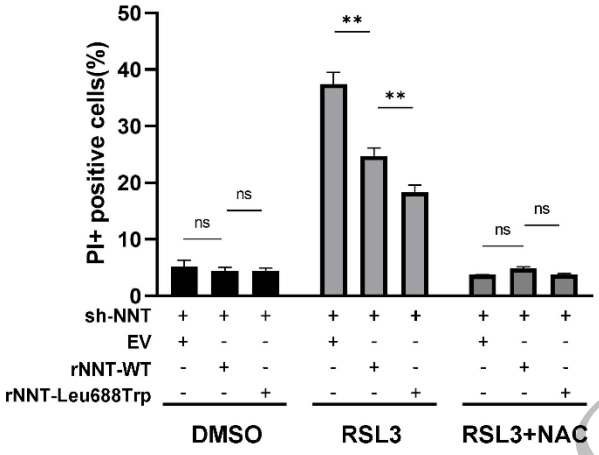

1

2 *Figure 5d*

3 *85x66 mm (DPI)*